

A surface structural model for ferrihydrite II: Adsorption of uranyl and carbonate

Tjisse Hiemstra^{a,*}, Willem H. Van Riemsdijk^{a,1}, André Rossberg^{b,2},
Kai-Uwe Ulrich^{c,3}

^a Department of Soil Quality, Wageningen University, P.O. Box 47, 6700 AA Wageningen, The Netherlands

^b Institute of Radiochemistry, Forschungszentrum Dresden-Rossendorf, P.O. Box 51 01 19, 01314 Dresden, Germany

^c Department of Energy, Environmental and Chemical Engineering, Washington University in St. Louis, CB 1180, St. Louis, MO 63130, USA

Received 9 December 2008; accepted in revised form 28 April 2009; available online 12 May 2009

Abstract

The adsorption of uranyl (UO_2^{2+}) on ferrihydrite has been evaluated with the charge distribution (CD) model for systems covering a very large range of conditions, i.e. pH, ionic strength, CO_2 pressure, U(VI) concentration, and loading. Modeling suggests that uranyl forms bidentate inner sphere complexes at sites that do not react chemically with carbonate ions. Uranyl is bound by singly-coordinated surface groups present at particular edges of Fe-octahedra of ferrihydrite while another set of singly-coordinated surface groups may form double-corner bidentate complexes with carbonate ions. The uranyl surface speciation strongly changes in the presence of carbonate due to the specific adsorption of carbonate ions as well as the formation of ternary uranyl-carbonate surface complexes. Data analysis with the CD model suggests that a uranyl tris-carbonato surface complex, i.e. $\equiv(\text{UO}_2)(\text{CO}_3)_3^{4-}$, is formed. This species is most abundant in systems with a high pH and carbonate concentration. This finding differs significantly from previous interpretations made in the literature. At high pH and low carbonate concentrations, as can be prepared in CO_2 -closed systems, the model suggests the additional presence of a ternary uranyl-monocarbonato complex. The binding mode (type A or type B complex) is uncertain. At high uranyl concentrations, uranyl polymerizes at the surface of ferrihydrite giving, for instance, tris-uranyl surface complexes with and without carbonate. The similarities and differences between U(VI) adsorption by goethite and ferrihydrite are discussed from a surface structural point of view.

© 2009 Elsevier Ltd. All rights reserved.

1. INTRODUCTION

Uranium (U) is a toxic element that is bioavailable and migrates in the environment. The migration depends on the distribution of uranium over the mobile and immobile phases. Uranium in the mobile phase may interact with mineral phases and organic matter (Davis et al., 2004; Van-

denhove et al., 2007). In the case of adsorption, the distribution over phases will depend on the type of surface complexes formed at the given solution chemistry. Therefore, surface speciation is a key factor in understanding and quantifying uranium migration in laboratory studies (Gabriel et al., 1998; Logue et al., 2004; Cheng et al., 2007) as well as at mining sites and nuclear waste repositories (Davis et al., 2004; Logue et al., 2004).

Under oxic aqueous conditions, uranium is present as U(VI) in uranyl (UO_2^{2+}). This species is bioavailable (Van denhove et al., 2007). In solution, UO_2^{2+} may hydrolyze and in contact with CO_2 , uranyl forms a variety of carbonate complexes (Guillaumont et al., 2003). Uranyl may also adsorb to various types of iron oxides (Payne et al., 1994; Rosentreter et al., 1998; Barnett et al., 2002; Logue et al.,

* Corresponding author. Fax: +31 317 41 9000.

E-mail addresses: tjisse.hiemstra@wur.nl (T. Hiemstra), willem.vanriemsdijk@wur.nl (Willem H. Van Riemsdijk), rossberg@esrf.fr (A. Rossberg).

¹ Fax: +31 317 41 9000.

² Fax: +33 476 88 2525.

³ Fax: +1 314 935 7211.

2004) that are ubiquitous in the natural environment. Ferrihydrite (Fh) or hydrous ferric oxide (HFO) is considered to be an important reactive phase, binding uranium in various surface complexes.

Ferrihydrite (Fh) can be used as a proxy for the natural reactive oxide fraction of soils and sediments. Ion binding by this mineral has been studied extensively (Dzombak and Morel, 1990). Modeling the adsorption behavior of Fh is very challenging since the surface structure, as well as its composition, is uncertain as discussed in Part I (Hiemstra and Van Riemsdijk, 2009). The surface structure is critical because ions form surface complexes of varying reactivity by interacting with different types of surface sites. A study of the interaction of Fh with uranyl in the presence and absence of carbonate ions can be used for better understanding the surface chemistry of Fh in general because the two ions are known for their different binding mechanisms. Uranyl ions are preferentially bound as a bidentate complex at the edges of Fe octahedra (Manceau et al., 1992) while carbonate ions form double-corner bidentate complexes (Hiemstra et al., 2004; Bargar et al., 2005).

The adsorption of uranyl can be studied with different approaches at different scales. Ideally, the processes identified at the microscopic scale can be used in the description of phenomena observed at the macroscopic scale. Processes taking place at the microscopic scale can nowadays be directly studied using modern in situ spectroscopic methods such as extended X-ray absorption fine structure spectroscopy (EXAFS) (Manceau et al., 1992; Waite et al., 1994) and Fourier transformed infrared (FTIR) spectroscopy (Wazne et al., 2003; Bargar et al., 2005; Ulrich et al., 2006). Different types of surface complexes have been proposed for the sorption of uranyl by Fe oxides. Dominant factors controlling the speciation are pH and the presence of CO₂. In the past, the EXAFS spectra derived from pure uranyl iron-oxide systems have usually been interpreted in terms of bidentate, edge sharing coordination (Manceau et al., 1992; Waite et al., 1994; Ulrich et al., 2006), but recently double-corner sharing has been suggested (Sherman et al., 2008). In the case of ternary surface complex formation between uranyl and carbonate, the number of CO₃²⁻ ions present in the UO₂²⁺ coordination sphere varies considerably between structural models. For hematite, surface complexes with one (Bargar et al., 1999) and two CO₃²⁻ ions (Bargar et al., 2000; Catalano et al., 2005) have been suggested. For goethite, the formation of a surface complex with only one CO₃²⁻ ion in the uranyl coordination sphere has been proposed (Sherman et al., 2008) and this has also been suggested for natural samples (Bostick et al., 2002). These ternary surface complexes are known as ‘type A’ complexes.

Surface complexation models (SCM) are tools that relate adsorption to equilibrium conditions in the aqueous phase. A large variety of SCM has been developed. These models have a thermodynamic basis, which implies that no particular knowledge about the molecular structure is required in order to describe the equilibrium relationship between solution and surface, i.e. hypothetical surface species can be used. This allows a great deal of flexibility in the assumed surface speciation. Therefore, the relationship

with the actual surface speciation is often unclear. An important complication is the dominant role played by electrostatic interactions at the solid–solution interface. These interactions are handled very differently in different SCMs, or are even not included at all (Morrison et al., 1995). This leads to significant differences in the calculated surface speciation. The challenge therefore is to construct a model that is able to link microscopic and macroscopic observations into a single coherent description of the interactions taking place.

A prerequisite for linking microscopic and macroscopic observations is the correct computation of the electrostatic energy contribution. It is now known that this cannot be calculated accurately by reducing the charge of an inner sphere complex to a single electrostatic point located near or at the surface. The main reason for this is that surface species experience the gradient in electrostatic potential in the compact part of the double layer. The charge distribution (CD) concept can be used to account for this phenomenon (Hiemstra and Van Riemsdijk, 1996). A CD value can be derived that describes the apportionment of the overall charge of an adsorbed species between different electrostatic ‘planes’. As described below, the CD concept is strongly linked to the molecular structure of surface complexes, hence it can provide a link between the microscopic and macroscopic descriptions. For a strong and convincing linkage, a critical interpretation of these CD values, obtained from data analysis, is necessary.

In a number of studies, different factors that influence the interfacial charge distribution have been identified. First of all, the interfacial CD value depends on the location of ligands in the compact part of the interface (Rietra et al., 1999). For instance, a bidentate surface complex will contribute more charge to the surface than a monodentate surface species because of the greater number of common ligands. Secondly, refinement of this principle is necessary where there is an asymmetry in the coordination sphere. This may be handled using the Brown bond valence concept (Brown, 2002) that relates the relative bond lengths to bond valence charge. In principle, the variation in bond length is experimentally accessible from spectroscopic tools but it can also be derived from geometric optimization using molecular orbital calculations (Hiemstra and Van Riemsdijk, 2006). The variation in bond length can rationalize the variation in CD values obtained for different metal ions such as Hg(II), Cu(II), Pb(II), and Cd(II). A third factor that may contribute to the interfacial charge distribution is the orientation of water molecules in the compact part of the electrostatic double layer (EDL) (Hiemstra and Van Riemsdijk, 2006). Water molecules tend to orient their dipole in the compact part of the interface depending on the surface charge. This orientation of the dipole charge reduces the effective charge separation created by ion adsorption, i.e. it is a (small) correction to the ionic charge distribution. Finally, the CD can also be affected by electron transfer as shown recently for the adsorption and surface oxidation of Fe(II) (Hiemstra and Van Riemsdijk, 2007).

In our first attempt to model the interaction of uranyl and carbonate with the CD model, we treated the surface

of ferrihydrite as homogeneous with only one type of site (i.e. singly-coordinated surface groups). However, this did not lead to a coherent and sufficiently satisfying description of uranyl adsorption over the full range of conditions, despite the high degree of freedom available in the choice of surface species. Introduction of an additional surface site (a triply-coordinated surface group) that only reacts with protons did not improve the fit.

Further exploration showed that it is essential to distinguish two types of sites that react with *either* uranyl or carbonate ions. The apparent absence of direct site competition suggests that the surface groups of the microscopic sites involved are physically separated on the surface. This observation has been the motivation for the development of a multisite ion complex (MUSIC) model for ferrihydrite despite its structural complexity and uncertainty as described in Part I (Hiemstra and Van Riemsdijk, 2009). In the present paper, the focus will be on ion adsorption using the CD model to relate macroscopic adsorption data to the microscopic structures observed by spectroscopy. The uranyl and carbonate ions are used since these ions may react differently with the surface and are environmentally important. We will evaluate the adsorption of uranyl by freshly prepared ferrihydrite using literature data from the most extensive studies (Hsi and Langmuir, 1985; Waite et al., 1994; Morrison et al., 1995; Payne, 1999). These cover a very broad range of conditions (pH, ionic strength, uranyl loading, carbonate concentration, and CO₂ partial pressure). The main objective is to improve our understanding of the surface reactivity of Fh in relation with ion adsorption, more than just obtaining a good description of the experimental data.

2. URANYL ADSORPTION DATA

The aqueous solution chemistry of uranyl is quite complex and includes many aqueous species (Guillaumont et al., 2003). Uranyl may be present as a cation (UO₂²⁺) at low pH but readily hydrolyzes to a series of mononuclear species such as UO₂OH⁺ and UO₂(OH)₂⁰. Uranyl also strongly interacts with carbonate ions. In seawater for instance, the dominant species is UO₂(CO₃)₃⁴⁻. Another feature is the extensive polymerization of uranyl in the concentration range just below the solubility of an important uranyl mineral, (meta-)schoepite (UO₂(OH)₂(s)). The speciation can be calculated using the reactions and thermodynamic data given in Table A1 of the Appendix, which are based on a critical selection of reactions and thermodynamic constants (Guillaumont et al., 2003). The auxiliary ion pair formation reactions with Na⁺, active at high ionic strength, have a minor effect on the aqueous U(VI) speciation, but might be realistic since the given log *K* values for U(VI) are for zero ionic strength.

2.1. Open and closed systems

Generally, the adsorption of uranyl (UO₂²⁺) is studied in two different types of systems. In many cases, the systems are open to the atmosphere leading to the presence of carbonate species. The use of open systems, equilibrated with

air, has the advantage that it more closely resembles natural conditions. However, the pH and carbonate concentration cannot be varied independently at a given CO₂ partial pressure. A high pH inevitably leads to a high carbonate concentration and vice versa. In other cases, closed systems containing a variable amount of carbonate have been used. In these cases, the uranyl speciation may be studied at high pH in combination with a relatively low concentration of carbonate. In such systems, an analysis of the adsorption data may be able to resolve surface species that cannot be resolved when their contribution is suppressed by high carbonate concentrations.

For ferrihydrite, freshly prepared and aged for 4 h, the first extensive study of uranyl adsorption in closed systems was carried out by Hsi and Langmuir (1985). The concentration range studied was subsequently extended by Morrison et al. (1995) who measured adsorption isotherms as well as adsorption edges for Fh aged for 24 h. The combined data set (*n* = 168 data points) is shown in Fig. 1 and covers a very wide range of conditions (loading, pH, and uranyl and carbonate concentrations). The adsorption of uranyl is strongly pH dependent (Fig. 1a and b) and dissolved U(VI) concentrations rapidly decrease above pH ~ 4. When carbonate is added, the total concentration of U(VI) in solution may increase as a result of desorption. This is most clearly seen at high pH. Uranyl desorption is mainly due to the formation of dissolved uranyl-carbonate complexes such as UO₂CO₃⁰ (aq), UO₂(CO₃)₂²⁻ (aq), and UO₂(CO₃)₃⁴⁻ (aq). Desorption of uranyl is counteracted by the adsorption of carbonate ions to the ferrihydrite surface. The binding of this anion lowers the positive charge of the particles leading to less electrostatic repulsion of UO₂²⁺. In addition, ternary uranyl-carbonate complexes may form at the surface and increase the loading. In systems with a high equilibrium U(VI) concentration, uranyl may polymerize. Polymerization may occur both in solution and at the surface. The above suggests that for a complete description of adsorption data, covering a wide range of conditions, one may anticipate the presence of a range of surface species. This is not surprising since a description of the solution chemistry already requires a large number (~20) of uranyl species (Table A1). Therefore, surface complexation modeling of uranyl is a challenge.

The adsorption of uranyl by ferrihydrite (aged 3 days at 25 °C) has also been studied for open systems (Waite et al., 1994). In the original paper, the data were presented as the fraction adsorbed (Fig. 2, left panels). With this traditional scaling, the adsorption is almost complete (~100%) over large parts of the pH range of relevance in nature. Much valuable information can be preserved if one uses the logarithms of the dissolved U(VI) concentrations (log *C*) instead. To do so, we have gone back to the original data presented in the PhD thesis of Payne (1999) and back-calculated the dissolved concentrations (*n* = 198 data points, Fig. 2, right panels).

Equilibrium concentrations rapidly decrease and show a strong pH dependency of adsorption (Fig. 2). They may reach a concentration range where the presence of any colloids remaining after phase separation could influence the apparent observed concentration. Low

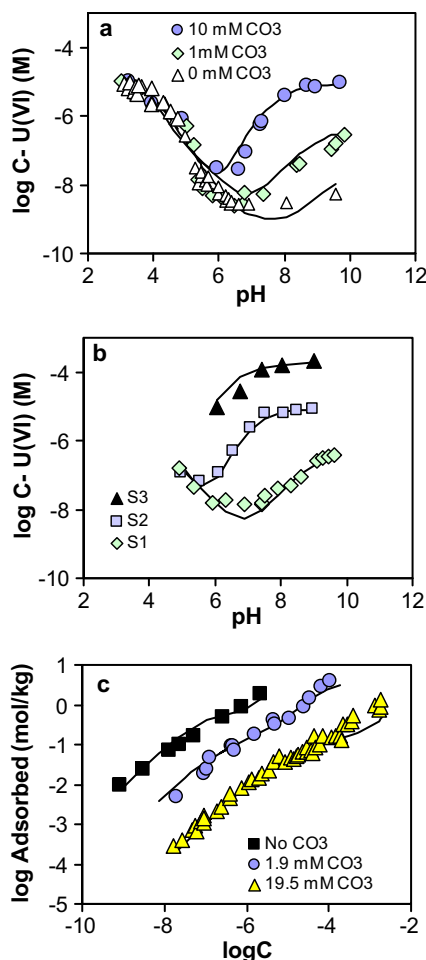


Fig. 1. Equilibrium concentrations of dissolved or adsorbed uranyl in closed systems with ferrihydrite and 0.1 M NaNO_3 . Symbols show experimental data obtained from the literature (168 data points), lines are calculated with the CD MUSIC model (this work). (a) The pH dependency of the uranyl adsorption in the absence and presence of carbonate for 1 g HFO/L and 10 μM U(VI) (Hsi and Langmuir, 1985). The pH dependency in (b) is for 1 mM CO_3^{2-} , 1 g HFO/L and 10 μM U(VI) (S 1) or 19.5 mM CO_3^{2-} , 0.52 g HFO/L and 8.4 μM U(VI) (S 2), or 19.5 mM CO_3^{2-} , 1 g HFO/L and 210 μM U(VI) (S 3) (Morrison et al., 1995). (c) Uranyl adsorption isotherms in closed systems for an increasing initial concentration of carbonate at pH = 7.0. The NaNO_3 electrolyte concentration is respectively 0.1, 0.1, and 0.08 M.

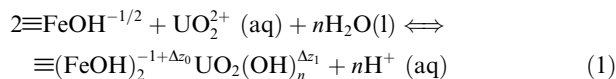
concentrations are also more easily influenced by ad/desorption from laboratory equipment such as reaction vessels, pipettes etcetera (Payne et al., 1998; Payne, 1999). This means that data for very low concentrations have to be assessed critically. Another point of concern is the exclusion of CO_2 , which must not only be done in the actual adsorption experiments but also during the preparation of the ferrihydrite, since a rapid and complete removal of carbonate is difficult to achieve, particularly at high pH. The exclusion of CO_2 during the ferrihydrite preparation has not been explicitly reported for the experiments analyzed in Fig. 1.

2.2. Uranyl surface complexation

The adsorption of uranyl on ferrihydrite has been studied with EXAFS by a number of authors (Waite et al., 1994; Dodge et al., 2002; Ulrich et al., 2006). The relatively short Fe–U distance (~ 341 pm) indicates that the uranyl ion is bound at the edge (^1E) of a Fe-octahedron (Manceau et al., 1992). A bidentate surface complex is formed in which two ligands in the equatorial plane of the uranyl ion are linked to a single octahedron of the ferrihydrite surface (Fig. 3a). The reported total number of equatorial –OH/ OH_2 ligands is usually 5, but for a uranyl tris-carbonate complex it will be 6.

It is important to realize that edges are exposed by octahedra on all surfaces but not all edges are suitable for the binding of uranyl. This can be illustrated for goethite. For instance, the iron octahedra at the 0 2 1 face (see Part I) of this mineral have edges that are a composite of one singly- ($\equiv\text{FeOH}$) and one doubly- ($\equiv\text{Fe}_2\text{OH}$) coordinated surface group and this combination is also present in Fig. 3a. At the 1 1 0 face of goethite, the edges can be a combination of one $\equiv\text{FeOH}$ and one $\equiv\text{Fe}_3\text{O}$ group. These edges are not reactive towards uranyl for at least steric reasons. As discussed later, uranyl (UO_2^{2+}) has a specific structure with two axial oxygens and 5 or 6 equatorial water ligands. One of the axial oxygens of uranyl prevents binding of uranyl to the above-mentioned edges because it would lead to a too large repulsion of the axial oxygen by the surface group. EXAFS data support this proposition for ferrihydrite, showing only one Fe atom at a distance of about 341 ± 2 pm while binding at such edges would probably lead to a second Fe in the coordination sphere at a distance of about 360–370 pm. We note that another edge on the 1 1 0 face, formed by two doubly-coordinated $\equiv\text{Fe}_2\text{OH}^0$ sites, does not have this steric problem, but we assume that these surface groups are nevertheless not reactive for binding uranyl because the oxygen charge of these surface groups is already adequately compensated by the associated proton.

If the surface groups of ferrihydrite that interact with UO_2^{2+} are singly-coordinated $\equiv\text{FeOH}^{-1/2}$ groups, the general formation reaction for edge-sharing can be written as:



where the value of $n = 0, 1, 2, \dots$. All surface species, defined by Eq. (1) with $n = 0-4$, have been allowed simultaneously in our modeling approach and the presence of any of these species has been accepted or rejected based on the standard deviation of the fitted log K value and improvement of the correlation coefficient (R^2). A high standard deviation suggests that a species does not contribute significantly to the description of the data. With three surface species ($n = 0, 1, 2$), uranyl adsorption in the absence of carbonate could be described for the entire pH range of pH = 3–10, but $\equiv(\text{FeOH})_2\text{UO}_2\text{OH}$ ($n = 1$) was found to be dominant. The final parameterization, described later in Section 4, has been done by fitting all

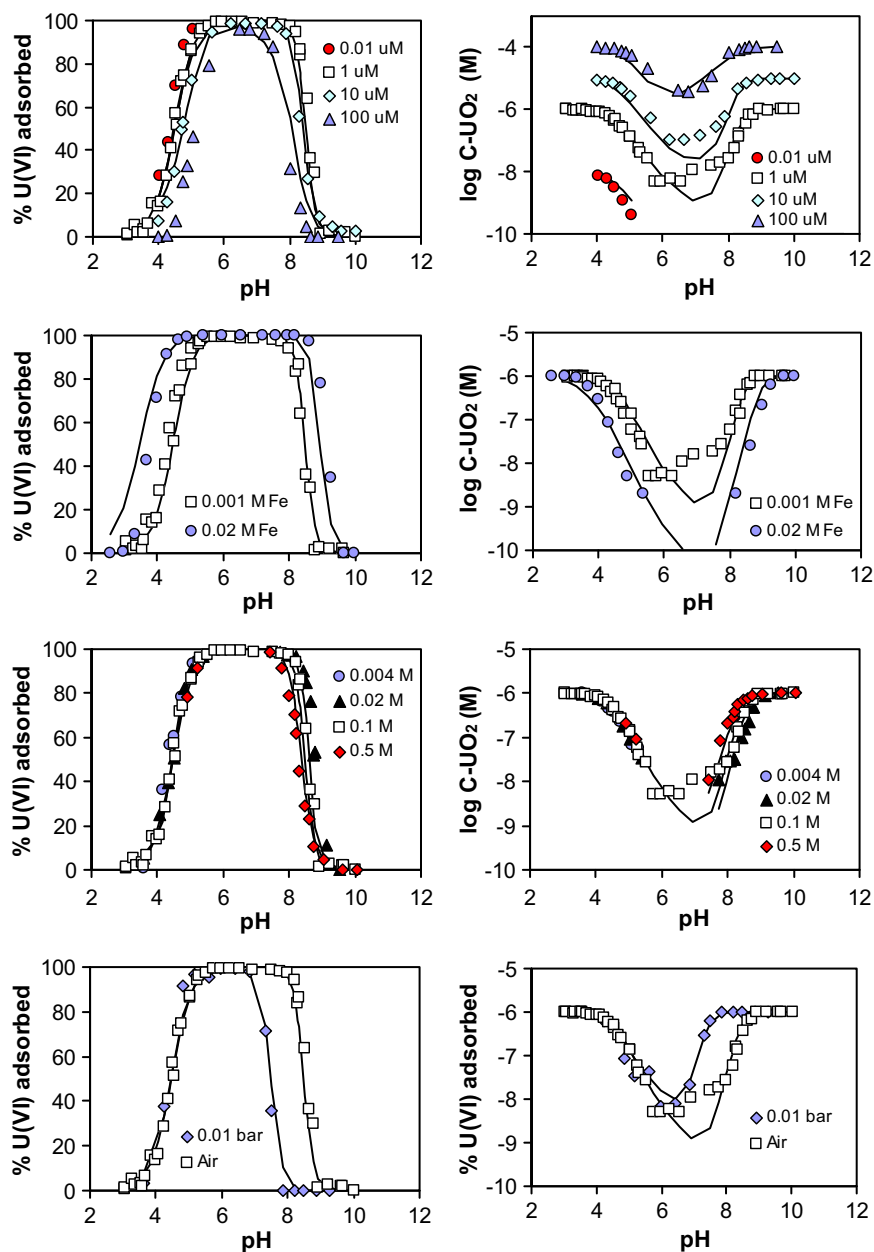


Fig. 2. The fraction of uranyl adsorbed to ferrihydrite as a function of pH (left panels) and the corresponding equilibrium concentrations (right panels). Data points are from Waite et al. (1994) and Payne (1999). The molar was set at $M = 102 \text{ g/mol Fe}$ and $A = 650 \text{ m}^2/\text{g}$. Lines are calculated with the CD MUSIC model (this work). From top to bottom, the systems show the effect of varying the initial U(VI) concentration (a and e), the ferrihydrite loading (b and f), the ionic strength (c and g), and the CO_2 partial pressure (d and h). All systems are based on 1 mM Fe, 0.1 M NaNO_3 , $p\text{CO}_2 = 0.365 \text{ mbar}$ and an initial U(VI) concentration of 1 μM , unless otherwise indicated in the figures.

168 data points of Fig. 1 simultaneously. Note that in the case of edge sharing, the Fe/U stoichiometry should not be read directly from the stoichiometry shown in the reaction (Eq. (1)) since the Fe ion in both surface reference groups ($\equiv\text{FeOH}^{-1/2}$) refers to the same Fe ion in the surface structure, i.e. the actual species is $\equiv\text{Fe}_{2/2}(\text{OH})_2\text{UO}_2(\text{OH})_n$.

In the CD model, a part of the charge of the adsorbed uranyl species is attributed to the surface (Δz_0), and the remaining part is attributed to the electrostatic 1-plane on

the other side of the Stern layer (Δz_1), see Part I (Hiemstra and Van Riemsdijk, 2009). For the above reaction, we may write $\Delta z_0 + \Delta z_1 = +2 - n$. The value $2 - n$ represents the net amount of charge added to the interface according to the adsorption reaction. This net amount of the charge ($2 - n$) is redistributed in the interface ($\Delta z_0 + \Delta z_1$). The charge distribution is essential if the aim is to describe the adsorption behavior using physically-realistic species. The quantification of the charge distribution is described in Section 3.

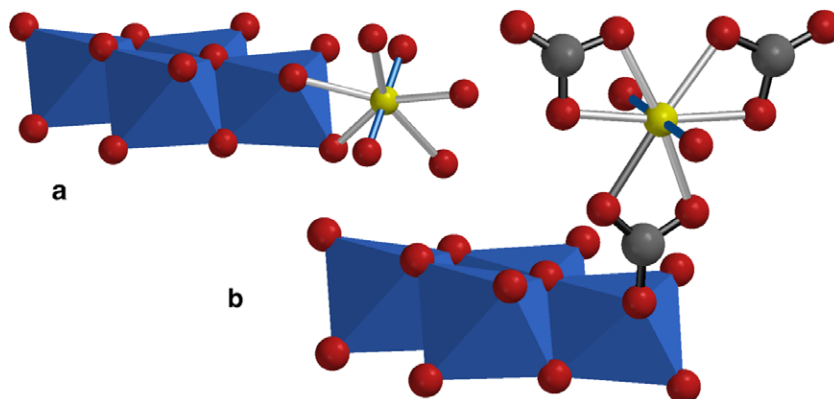
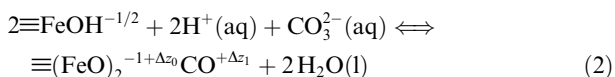


Fig. 3. Representation of the most prominent uranyl surface complexes in open systems, i.e. uranyl (a) bound by two singly-coordinated surface groups present at a free edge (protons not shown). For this geometry with $d(\text{Fe}-\text{U}) = 345$ pm and $d(\text{U}-\text{O}_{\text{edge}}) = 249$ pm, $d(\text{O}-\text{O})_{\text{edge}}$ is ~ 287 pm. The outer ligands of the uranyl surface complex in (a) may be OH, OH₂, or CO₃ (not shown). (b) A uranyl tris-carbonato complex that is singly-coordinated to an Fe ion in the solid via a carbonate group (a ternary type B complex).

2.3. Uranyl-carbonate surface complexation

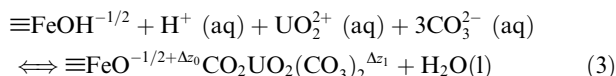
In the presence of carbonate, the behavior of the system will change due to the binding of carbonate ions that interact electrostatically with the adsorbed uranyl, i.e. the above $\equiv(\text{FeOH})_2\text{UO}_2(\text{OH})_n$ species (Eq. (1)). Carbonate ions may form double-corner (²C) bidentate inner sphere complexes (Hiemstra et al., 2004; Bargar et al., 2005). The reaction can be written as:



in which $\Delta z_0 + \Delta z_1 = +2 - 2 = 0$ (sum of charge of adsorbing and desorbing species). Adsorbed carbonate is negatively-charged and so will stimulate the binding of cations such as UO_2^{2+} . This interaction has been omitted for imogolite (Arai et al., 2006) but it may affect the choice of any additional ternary surface species. The presence of carbonate also leads to the formation of uranyl-carbonate complexes in solution. This will decrease the activity of free $\text{UO}_2^{2+}(\text{aq})$ and consequently suppress uranyl adsorption. If only the basic inner sphere sorption species of Eq. (1) and Eq. (2) are considered in the SCM, the predicted equilibrium concentrations of dissolved U(VI) are too high compared with the experimental data. This suggests that a ternary uranyl-carbonate species is present at the surface, but which species will this be?

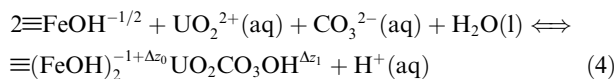
Preliminary modeling showed that the uranyl adsorption data of Fig. 2a–d (open systems) could be described rather well by assuming the formation of a single type of ternary U(VI)-carbonato surface complex. This species must contain a large number of carbonate ions in order to be able to reproduce the observed data. A uranyl tris-carbonato ($\text{UO}_2(\text{CO}_3)_3^{4-}$) complex was found to be a very good candidate. The pH dependency of the adsorption of this species is largely controlled by the CD value (see Section 3), which is related to the specific coordination mode, outer- or inner-sphere, mono- or bidentate. The precise binding mode is insufficiently clear from the analysis of the open systems presented in Fig. 2a–d in which both pH and carbonate

concentration are coupled, but can be resolved with later CD-modeling. If singly-coordinated surface groups are involved in the formation of a ternary type B monodentate inner sphere complex (Fig. 3b), the reaction can be described as:



in which $\Delta z_0 + \Delta z_1 = \text{net charge added} = -3$ v.u. (valence unit). We note that the stoichiometry of an outer sphere complexation reaction involving uranyl tris-carbonato (i.e. formation of $\equiv\text{FeOH}_2^{+1/2}-\text{UO}_2(\text{CO}_3)_3^{4-}$) will be the same as defined above apart from the release of a water molecule due to ligand exchange. The major difference in terms of modeling is the difference in the interfacial charge distribution for the two types of complexes. In the case of inner sphere complexation, more charge (negative) is transferred to the surface and less to the 1-plane, see Fig. 3 in Part I (Hiemstra and Van Riemsdijk, 2009). Therefore, the fitted CD values may be used to test which option is the more likely. This will be discussed in detail later (Section 4).

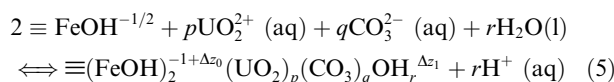
The above adsorption reactions (Eqs. 1, 2, 3) have been used to describe the data collected for the closed systems shown in Fig. 1. A good description is found for systems with high carbonate loading, but the U(VI) concentration is significantly over-predicted for systems with a high pH ($\text{pH} \geq 7-8$) and a low carbonate loading (initially 1 mM CO₃). The latter conditions are considerably different from those observed in the open systems of Fig. 2 where a high pH inevitably leads to a high carbonate concentration. The over-prediction of the equilibrium concentration points to the formation of one or more additional ternary uranyl-carbonate surface complexes containing a smaller number of carbonate ions. We found that the description of adsorption in these closed systems could be improved by introducing a hydrolyzed uranyl surface species that binds just one carbonate ion, i.e. $\equiv(\text{FeOH})_2\text{UO}_2\text{CO}_3\text{OH}$. The formation reaction for such a (ternary type A) uranyl-monocarbonato complex is:



with $\Delta z_0 + \Delta z_1 = -1$ v.u. This species may be protonated at low pH. As will be explained in Section 4, the selection of this species and the corresponding reaction stoichiometry have been constrained by the choice of a CD value that is based on the structure of such a uranyl surface complex. Other alternatives are also discussed.

2.4. Polymerization

The adsorption isotherms in the closed systems of Fig. 1c have been determined over a very large range of concentrations that reach at their upper limits the solubility of $\text{UO}_2(\text{OH})_2(\text{s})$ minerals. The amount of data at large uranyl concentrations is limited and the number of possible complexes is high. For this reason, an unambiguous identification of the type of complexes that may form is difficult. Polymerization can be described by a general formation reaction, including polymer adsorption with and without ($q = 0$) carbonate adsorption:



with $\Delta z_0 + \Delta z_1 = 2p - 2q - r$. As will be discussed in the modeling section, the stoichiometric coefficients (p, q, r) have been selected by trial and error but in all cases the choice has been constrained by their ability to give a realistic set of CD values.

3. CHARGE DISTRIBUTION

Surface complexes are relatively large and their charge is spatially distributed in the compact part of the double layer as shown in Fig. 3 of Part I (Hiemstra and Van Riemsdijk, 2009). Near the surface, a steep gradient in the electrostatic potential exists. The energy of adsorption is partly controlled by the surface potential but is also partly related to the potential further away from the surface. This is the basis of the charge distribution (CD) model (Hiemstra and Van Riemsdijk, 1996). In calculations with the CD model, one part of the charge of an inner sphere complex is attributed to the electrostatic surface plane (0-plane), while the other part is located in an electrostatic plane (1-plane) at some distance from the surface. The charge of the outer sphere complexes of electrolyte ions is entirely attributed to the 1-plane (see Fig. 3 of Hiemstra and van Riemsdijk (2009)).

In principle, the interfacial charge distribution ($\Delta z_0, \Delta z_1$) of a surface complex may be derived from an analysis of adsorption data. The CD values not only strongly regulate the pH dependency of adsorption, but they also strongly affect the ion-ion competition (Hiemstra and Van Riemsdijk, 1999; Stachowicz et al., 2006, 2008). However, a complicating factor is that the pH dependency is also influenced by the hydrolysis of surface species. Therefore, we prefer to estimate the CD value based on the geometry of the surface complex where possible.

In the simplest approach, one may assume a 1:1 relationship between the interfacial ligand and the charge distribution and apply the Pauling Bond valence concept (Rietra et al., 1999). In the case of an uranyl bidentate surface complex with two axial oxygens and five equatorial oxygens, an equal distribution of the U(VI) charge over all ligands will lead to a Pauling bond valence of $v = z/\text{CN} = 6/7 = 0.86$ v.u. (valence unit). Since two such bonds are formed with the surface, the surface charge attribution will be twice this value, i.e. $\Delta z_0 \sim 1.7$ v.u. The corresponding value of Δz_1 will be 0.3 v.u. since $\Delta z_0 + \Delta z_1 = +2$ v.u. in the case of UO_2^{2+} adsorption. However, the Δz_0 and Δz_1 values of the Pauling approach are unlikely because in practice the charge is not equally distributed over the coordination sphere. Uranyl is a typical example of an ion with an asymmetric distribution of the bond valence charge. The two axial-oriented oxygens with the short U–O bond (~ 180 pm) neutralize a large part of the U(VI) charge. The remainder will be distributed over the equatorial oxygens and is relatively small, resulting in weaker and longer U–O bonds. According to Brown (Brown, 2002), the relation between the bond length R and the actual bond valence or bond strength s is given by:

$$s = e^{-(R-R_0)/B} \quad (6)$$

where B is a constant. The value of the element-specific distance parameter R_0 is chosen such that the sum of the Brown bond valences equals the formal valence of U(VI) ($\sum s_j = 6$). Usually, the value of B is set equal to 37 pm (Brown and Altermatt, 1985). In general, this choice leads to a good description of the variation of the bond valence as a function of bond length for many elements. However, in the case of uranyl, a much better description of the structure of the U(VI) minerals is found with $B = 52$ pm (Burns et al., 1997). The higher value of B indicates that coordinating oxygens, present at larger distances, contribute more to the neutralization compared with the oxygens around light elements. This points to an alternative electronic structure for U(VI).

EXAFS data for uranyl adsorbed to ferrihydrite (Waite et al., 1994; Dodge et al., 2002; Ulrich et al., 2006) show the presence of three U–O distances. Besides the short axial bond, two U–O bond lengths are found for the oxygens in the equatorial plane, which are about 233 ± 2 pm and 249 ± 5 pm (Table 1). All three distances represent different bond valence values. If uranyl is bound to the surface via two short equatorial U–O bonds, the corresponding ionic charge contribution to the surface is $n_0 = 1.2$ v.u. based on Eq. (6), while it is $n_0 = 0.9$ v.u. if two long equatorial U–O bonds are present. Recently, the geometry of $\equiv(\text{FeOH})_2\text{—UO}_2\text{—}(\text{OH})_3$ has been optimized (Sherman et al., 2008) with molecular orbital (MO) computations using density functional theory (DFT). The equatorial U–O distances of the adsorbed $\equiv\text{UO}_2^{2+}$ are very similar and relatively large, i.e. 245 ± 3 pm. A (much) shorter U–O distance (215 pm) in the coordination sphere results if a —OH_2 ligand deprotonates to —OH (Oda and Aoshima, 2002). Coordination with CO_3^{2-} also leads to shorter MO/DFT-calculated U–O distances. For this reason, we assume that the U–O bonds to the metal ions in the solid are relatively

Table 1

The coordination numbers (CN) and experimental bond distances (R , pm) reported in the literature for U(VI) complexation by ferrihydrite in the absence of CO_2 measured using EXAFS, which are used to calculate the ionic charge distribution (n_0, n_1) assuming bidentate complex formation. Two strong axial bonds are formed and 5 weaker equatorial bonds. Note $\Sigma(\text{CN}) = 7$. $R_0 = 206 \pm 2$ nm.

Reference	CN	$R_{\text{U-O}}$	n_0	n_1
Waite et al. (1994)	2	180		
	3	235		
	2	252	0.85	1.15
Dodge et al. (2002)	2	179		
	3	235		
	2	254	0.81	1.19
Ulrich et al. (2006)	2	179		
	2	229 ^a		
	3	241 ^a	0.99	1.01

^a In the case of an equal distribution in the equatorial plane, $n_0 = 1.12$ and $n_1 = 0.88$ v.u.

long (Fig. 3a) and that hydrolysis and/or carbonate binding is responsible for the relatively short U–O bonds observed. A long distance for the U–O-surface bonds was also proposed by Waite et al. (1994). The value of R_0 of U(VI) obtained for the structures of the various complexes is 206 ± 2 pm.

The CD values for the above geometric model can be estimated by using the U–O distances (R) and CN values (Table 1) reported for ferrihydrite in the various EXAFS studies (Waite et al., 1994; Dodge et al., 2002; Ulrich et al., 2006). The interfacial surface charge contribution (Δz_0) results from an ionic contribution (n_0) and a possible correction due to dipole orientation (Hiemstra and Van Riemsdijk, 2006). For the ionic charge contribution to the surface, the application of the Brown bond valence equation (Eq. (6)) results in a value of $n_0 = 0.88 \pm 0.09$ v.u. for the long bonds between U(VI) and the surface oxygens (Table 1). The uncertainty in the ionic charge distributions, n_0, n_1 (Table 1), are greater than any effect due to changes in the water dipole orientation caused by the reaction (Hiemstra and Van Riemsdijk, 2006). This is calculated as $\sim +0.02$ v.u. in this case. The interfacial surface charge contribution used in our calculations is set at $\Delta z_0 = 0.9$ v.u. for all bidentate surface species in which the uranyl is linked to the surface ($\Delta z_0 \approx n_0$). We note that in a free fit, one finds $\Delta z_0 = 0.81 \pm 0.08$ v.u. which is in line with the above estimated CD value. However, the use of a higher CD value ($\Delta z_0 = 1.2$ v.u., i.e. shorter U–O bonds with the surface) in the final modeling resulted in only a slightly lower quality of the fit ($R^2 = 0.975$) than the use of $\Delta z_0 = 0.9$ v.u. ($R^2 = 0.977$). It is interesting to note that the above-derived CD value of 0.90 v.u. is close to a Pauling distribution of the charge (+2 v.u.) of UO_2^{2+} over the equatorial ligands, i.e. assuming that the axial oxygens of UO_2^{2+} are fully neutralized. This leads to $v = z/\text{CN} = 2/5$ and in case of bidentate formation $\Delta z_0 = 0.8$ v.u. and $\Delta z_1 = 1.2$ v.u.

Recently, the CD approach has been used as fitting tool to describe uranyl adsorption on goethite (Sherman et al.,

2008). The authors attributed all uranyl charge to the 0-plane ($\Delta z_0 = +2$ v.u.) and therefore treated it as a single point charge. In our opinion, this is difficult to reconcile with the structure discussed above in which the charge attributed to the surface charge is based on the number of common ligands and the corresponding bond valence (Eq. (6)). A negative value of Δz_0 ($\Delta z_0 = -1.1$ v.u.) has been proposed for the formation of a uranyl inner sphere complex ('type A' complex) at the surface of imogolite (Arai et al., 2006). This is obviously in conflict with any structural interpretation based on the CD approach.

4. MODELING URANYL SURFACE COMPLEXATION

In general, the mutual interaction of ions bound at charged surfaces is dominantly regulated by electrostatics. The site saturation is usually an effect of second order and only relevant at high loading. Our modeling is based on relative surface concentrations defined by mole fractions θ using for each type of site the corresponding site density as reference (Hiemstra and Van Riemsdijk, 1996). This definition results in a probability function $(\theta_{\text{FeOH}})^m$ in the expression for the mixing entropy. For bidentate formation, often a value $m = 2$ is used in the equilibrium expression, i.e. $(\theta_{\text{FeOH}})^2$. Monte Carlo simulations show (Hiemstra and Van Riemsdijk, 1990) that this mass action factor $(\theta_{\text{FeOH}})^2$ is applicable to a microscopic adsorption site with two surface groups that react as a unit to form a bidentate complex as found at the edge of an octahedron. However, if sites are present in rows, the microscopic ion adsorption site for bidentate formation can be formed by two different combinations of adjacent surface groups leading to another mixing entropy factor with $m < 2$ (LaViolette and Redden, 2002). These effects will only play a role at a very high loading. For practical reasons, we have used in all cases for the monodentate reactions $m = 1$ and for the bidentate reactions $m = 2$, see Table 2.

The model calculations have been done using a recent version of ECOSAT program (Keizer and Van Riemsdijk, 1998) in combination with FIT (Kinniburgh, 1993). The Davies equation with $C = 0.2$ was used for activity corrections. As discussed in Part I, ion adsorption on nanoparticles can be described well using the flat diffuse double layer theory in combination with a Stern layer capacitance ($C = 1.15 \text{ F/m}^2$) that is based on the theory for spherical condensers.

4.1. Carbonate interaction

Before modeling the uranyl-carbonate interaction, the adsorption of carbonate alone must be described. To our knowledge, the only carbonate adsorption data available for ferrihydrite are those published by Zachara et al. (1987) and shown in Fig. 4. These data can be described by assuming carbonate interaction with specific singly-coordinated surface groups ($N_s(c) = 3.5 \text{ nm}^{-2}$) that lead to the formation of double-corner complexes (Eq. (2)). The uncertainty in the data is quite high. Therefore, only the log K value has been fitted (Table 2). The CD value of this complex has been taken from Rahnemaie et al. (2007), who

Table 2

Tableau defining the formation of the surface species of uranyl and carbonate with the corresponding log K values and standard deviation (\pm) found by fitting the data of Fig. 1 ($n = 168$ observations covering a large range of conditions).

Species	$\equiv\text{FeOH}(\text{e})^{\S}$	$\equiv\text{FeOH}(\text{c})^{\#}$	Δz_0	Δz_1	Δz_2	H^+	UO_2^{2+}	CO_3^{2-}	log K
$\equiv(\text{FeO})_2 \text{CO}$	0	2	0.62 ^b	-0.62	0	2	0	1	+21.50 \pm 0.03
$\equiv(\text{FeOH})_2 \text{UO}_2$	2	0	0.9 ^c	1.1	0	0	1	0	+9.0 \pm 0.1
$\equiv(\text{FeOH})_2 \text{UO}_2\text{OH}$	2	0	0.9 ^c	0.1	0	-1	1	0	+3.30 \pm 0.06
$\equiv(\text{FeOH})_2 \text{UO}_2(\text{OH})_2$	2	0	0.9 ^c	-0.9	0	-2	1	0	-5.3 \pm 0.3
$\equiv(\text{FeOH})_2 \text{UO}_2\text{CO}_3\text{OH}^{\text{e,f}}$	2	0	0.9 ^c	-1.9	0	-1	1	1	+10.49 \pm 0.07
$\equiv\text{FeOCO}_2 \text{UO}_2(\text{CO}_3)_2$	0	1	0.33 ^d	-3.33	0	1	1	3	+36.63 ^a \pm 0.04
$\equiv\text{FeOCO}_2 \text{UO}_2(\text{CO}_3)_2$	1	0	0.33 ^d	-3.33	0	1	1	3	+36.63 ^a \pm 0.04
$\equiv(\text{FeOH})_2(\text{UO}_2)_3(\text{OH})_6$	2	0	0.9 ^c	-0.9	0	-6	3	0	-15.8 \pm 0.5
$\equiv(\text{FeOH})_2(\text{UO}_2)_3(\text{OH})_3\text{CO}_3$	2	0	0.9 ^c	0.1	0	-3	3	1	+14.6 \pm 0.2

[§] Singly-coordinated group $\equiv\text{FeOH}(\text{e})$ is able to form complexes by edge sharing, $N_s(\text{e}) = 2.5 \text{ nm}^{-2}$.

[#] Singly-coordinated group $\equiv\text{FeOH}(\text{c})$ is able to form double-corner complexes, $N_s(\text{c}) = 3.5 \text{ nm}^{-2}$.

^a The log K values of both monodentate complexes were kept equal during the fit.

^b Taken from Rahnamaie et al. (2007).

^c The Δz_0 value of all U(VI) bidentate edge complexes have been set equal to the value calculated from the Brown bond valence analysis. The value of Δz_1 is the difference between the total added charge and Δz_0 .

^d The CD value has been calculated assuming a Pauling bond valence charge distribution for the carbonate ion. If fitted, $\Delta z_0 = 0.30 \pm 0.15$ and $\Delta z_1 = -3.30$, see text.

^e The OH ligand of this species may protonate resulting in $\equiv(\text{FeOH})_2\text{UO}_2\text{CO}_3$. If included in the data description, log $K = 16.6 \pm 0.7$.

^f An alternative ternary uranyl mono-carbonato surface species is, $\equiv(\text{FeO}(\text{c}))_2\text{CO UO}_2(\text{OH})_3$. See text.

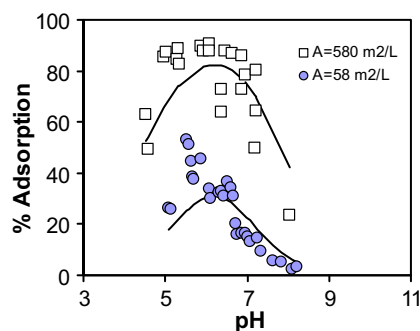


Fig. 4. The fractional carbonate adsorption in 0.1 M NaNO_3 with an initial concentration of $4.6 \mu\text{M}$ total carbonate in a system with 58 and 580 m^2 ferrihydrite/L. Data are from Zachara et al. (1987). The lines have been calculated using the parameters given in Table 2 and Part I (Hiemstra and Van Riemsdijk, 2009).

calculated this value from the MO/DFT optimized geometry of the complex.

4.2. Uranyl adsorption

As pointed out above, modeling of the uranyl adsorption in the closed systems is most conclusive because of the absence of a direct link between pH and carbonate concentration in the solution enabling the collection of data for low carbonate concentrations but a high pH. Systems not containing any carbonate are also useful since these allow the basic uranyl surface speciation and corresponding affinity constants (Eq. (1)) to be determined without the additional complexity of carbonate binding.

4.2.1. Uranyl tris-carbonato surface complex

Our initial modeling strongly suggested that a uranyl tris-carbonato surface complex contributes to the binding

of uranyl. Using this species, a large part of the data can be described well, including data at high pH and high carbonate concentrations. However, the precise linkage of this species to the surface (i.e. the CD value) is uncertain and so has been assessed by trying different options, e.g. formation of an outer sphere complex ($\equiv\text{FeOH}_2^{+1/2}-\text{UO}_2(\text{CO}_3)_3^{4-}$) and a monodentate inner sphere complex ($\equiv\text{FeO}-\text{CO}_2\text{UO}_2(\text{CO}_3)_2$). The focus is on the estimation of the CD value. In the case of outer sphere complex formation, the proton charge that is involved in the reaction to form $\equiv\text{FeOH}_2^{+1/2}$ is attributed entirely to the surface, i.e. $\Delta z_0 = +1$ v.u., and the charge of the uranyl tris-carbonato complex is attributed to the 1-plane, i.e. $\Delta z_1 = -4$ v.u. In the case of monodentate inner sphere complex formation, the water molecule is removed and replaced by one of the ligands of carbonate (Eq. (3), Fig. 3b). The corresponding amount of charge of that ligand ($=z_{\text{Oxygen}} + v = -2 + 1.33 = -0.67$ v.u.) is transferred from the 1-plane to the 0-plane leading overall to $\Delta z_0 = +1 - 0.67 = +0.33$ and $\Delta z_1 = -4 + 0.67 = -3.33$ v.u. This calculation shows that the value of Δz_0 ranges between $\Delta z_0 = +0.33$ v.u. (inner sphere complexation) and $\Delta z_0 = +1$ v.u. (outer sphere complexation). After optimization of the parameters in the final fit, we also searched for the CD value for this complex as a test of the consistency of the model. The free-fitted CD value was $\Delta z_0 = 0.31 \pm 0.15$ v.u. showing that the formation of a monodentate inner sphere complex might be considered as the more likely of these two options. Additional support comes from the fitted value of the affinity constant which is log $K \sim 7.9$ for the reaction $\equiv\text{FeOH}_2^{+1/2} + \text{UO}_2(\text{CO}_3)_3^{4-}(\text{aq}) \leftrightarrow \equiv\text{FeOH}_2^{+1/2}-\text{UO}_2(\text{CO}_3)_3^{4-}$. This log K value is unusually high for outer sphere complexation. It is important to note that in principle the uranyl tris-carbonato complex may form by interacting with all singly-coordinated surface

groups, i.e. FeOH(e) and FeOH(c) (Table 2). This approach has been used here.

It is possible to define an additional proton and surface group in the reaction for the formation of the uranyl tris-carbonato complex and to derive the CD values by fitting. This reaction is equivalent to the formation of e.g. a bidentate outer sphere complex such as $\equiv(\text{FeOH}_2)_2^{+1}\text{—UO}_2(\text{CO}_3)_3^{4-}$ or a bidentate inner sphere complex such as $\equiv(\text{FeO})_2\text{—CO—UO}_2(\text{CO}_3)_2$. The use of this reaction stoichiometry leads to almost the same quality of the fit, but the fitted Δz_0 value ($\Delta z_0 = 1.39 \pm 0.14$ v.u.) is difficult to reconcile with a reasonable surface structure. If the species is an outer sphere complex, we expect $\Delta z_0 = +2$ v.u. and in the case of an inner sphere complex, we expect $\Delta z_0 = +0.67$ v.u. These values are quite different from the fitted value. Actually, we observe that the charge of the additional proton in the reaction is almost completely attributed to the surface, similarly as demonstrated for carbonate in a previous study (Hiemstra et al., 2004). So, the fitted value of Δz_0 is much higher with an extra proton in the reaction. However, the corresponding Δz_1 value remains almost the same ($\Delta z_1 = -3.39$ v.u. instead of -3.31 v.u.). This shows that the model is particularly sensitive to the charge in the 1-plane. As pointed out in other papers (Hiemstra and Van Riemsdijk, 1999; Stachowicz et al., 2006, 2008), the potential of the 1-plane is critical in controlling the competition between species.

The above analysis shows that the CD model can be used as a pure fitting tool but this can lead to CD values that are not consistent with the supposed or measured structure of the chosen surface species. If the goal is to link macroscopic data to the microscopic picture, CD values should be used that are consistent with the structure of those complexes.

4.2.2. Uranyl mono-carbonato surface complex

Special attention has also been paid to the choice of other possible ternary uranyl-carbonate surface complexes that may help to explain the U(VI) adsorption especially at low carbonate concentrations (Eq. (4)). This choice is based on the best value of the CD coefficients. In principle, two different types of ternary complexes can be formed from uranyl and carbonate. The complex can be considered as the attachment of a CO_3 to an adsorbed uranyl species (type A) or the attachment of a uranyl ion to adsorbed carbonate ions (type B). If in both cases a bidentate complex is formed, the location and type of singly-coordinated surface groups involved are different (FeOH(e) or FeOH(c)). Apart from water, for the chosen stoichiometry (Eq. (4)), the complexes are either $\equiv(\text{FeOH})_2\text{UO}_2\text{CO}_3\text{OH}$ (type A) or $\equiv(\text{FeO})_2\text{COUO}_2(\text{OH})_3$ (type B). We have tested the most likely option by fitting the CD value based on these two options.

For the edge surface complex $\equiv(\text{FeOH})_2\text{UO}_2\text{CO}_3\text{OH}$, this leads to $\Delta z_0 = 0.98 \pm 0.11$ v.u. and $\Delta z_1 = -1.98$ v.u. Within the fitting error, the fitted value for Δz_0 is almost equal to the estimated CD value derived from a structural analysis of uranyl complexes ($\Delta z_0 \approx n_0 = +0.9$ v.u. based on Table 1). Therefore, we consider the chosen surface structure of the complex as realistic and supported by the data. It is possible that $\equiv(\text{FeOH})_2\text{UO}_2\text{CO}_3\text{OH}$ may pro-

tonate at low pH. Introduction of this species resulted in only a minor improvement in the quality of the fit ($R^2 = 0.977$) and the formation constant has a relatively large uncertainty associated with it ($\log K = 16.6 \pm 0.7$). For this reason, this species has not been included in the final fit but its presence cannot be excluded at low pH.

The UO_2^{2+} , CO_3^{2-} , and H^+ reaction stoichiometry as given in Eq. (4) in combination with $\equiv\text{FeOH(c)}$, is also consistent with the formation of a $\equiv(\text{FeO})_2\text{COUO}_2(\text{OH})_3$ (type B) surface complex. The expected CD value is $\Delta z_0 = 0.67$ v.u. and $\Delta z_1 = -1.67$ v.u. These values are only slightly different from the CD value for $\equiv(\text{FeOH})_2\text{UO}_2\text{CO}_3\text{OH}$, i.e. $\Delta z_0 = 0.9$ v.u. and $\Delta z_1 = -1.9$ v.u. The adsorption can be described almost equally well with the type B complex ($\log K = 10.47 \pm 0.06$) using $\Delta z_0 = 0.67$ v.u. A free fit of the CD value gives $\Delta z_0 = 0.86 \pm 0.11$ v.u., which deviates from the Pauling bond valence value ($\Delta z_0 = 0.67$ v.u.), but the resolution of the model is maybe not high enough to discriminate definitively between these two options. However, the comparison of both species, i.e. $\equiv(\text{FeOH})_2\text{UO}_2\text{CO}_3\text{OH}$ and $\equiv(\text{FeO})_2\text{COUO}_2(\text{OH})_3$, raises the question as to why uranyl in the latter species would have a strongly intensified hydrolysis? The hydrolysis is much stronger than found for adsorbed uranyl (Eq. (1)), which is mainly present as $\equiv(\text{FeOH})_2\text{UO}_2\text{OH}$. For this reason, we consider the formation of $\equiv(\text{FeOH})_2\text{UO}_2\text{CO}_3\text{OH}$ as the more likely reaction.

4.2.3. Uranyl bis-carbonato surface complex

With the choice of the combination of the uranyl tris-carbonato and mono-carbonato surface complex, it is not possible to improve the fit by introducing an additional uranyl bis-carbonato complex. When we excluded the formation of uranyl tris-carbonato surface species and used only a combination of mono- and bis-carbonato (type B) surface species, the best description was found for the combination of $\equiv(\text{FeOH})_2\text{UO}_2\text{CO}_3$ and $\equiv(\text{FeOH})_2\text{UO}_2(\text{CO}_3)_2$. However, the quality of the fit to the data in Fig. 1 is much lower ($R^2 = 0.95$) and systematic deviations exist.

4.2.4. Adsorbed uranyl polymers

At high loading, uranyl may polymerize and bind to iron oxide surfaces as found for hematite by EXAFS (Bargar et al., 2000). As mentioned above, the amount of relevant data is quite limited and this makes the choice of the surface species somewhat arbitrary. Two different types of uranyl polymers have been considered, with and without carbonate. We have assumed that the polymers are bound to the surface via edge binding of a uranyl moiety, i.e. the surface charge contribution has been fixed at $\Delta z_0 = 0.9$ v.u. In solution, di- and tri-uranyl polymers can be found (see Table A1 in the Appendix). These two options have been tried for the surface complexation reactions, i.e. $p = 2$ or 3 in Eq. (5). The number of OH groups was derived by changing the values of q and r in the reaction and searching for the best fit. The best description was found assuming the formation of $\equiv(\text{FeOH})_2(\text{UO}_2)_3(\text{OH})_6$ ($p = 3, q = 0, r = 6$) and $\equiv(\text{FeOH})_2(\text{UO}_2)_3(\text{OH})_5 \text{CO}_3$ ($p = 3, q = 1, r = 5$). Of

course, other polymer complexes might be present but no attempts have been made to resolve these.

4.2.5. Final modeling results

The closed systems in the experiments of Fig. 1 have a non-zero headspace. This implies that some of the added carbonate will enter the gas phase at low pH. This process has been included in the modeling using a gas/solution ratio of $V_{\text{gas}}/V_{\text{sol}} = 0.2 \text{ L/L}$, which is close to the average reported. About 10% of the carbonate may enter the gas phase (Jang et al., 2007). The final set of fitted parameters is given in Table 2 and the calculated results are given in Fig. 1a–c as lines. The overall quality of the fit is good ($R^2 = 0.977$). The root mean square error (RMSE) of the logarithm of the U(VI) concentrations is 0.23.

The standard deviation (SD) of the fitted log K value has been used in the modeling as one of the tools to judge the relevance of the various species for the data description (Table 2). In the absence of carbonate, the $\equiv(\text{FeO-H})_2\text{UO}_2\text{OH}$ species is most important. This species has the lowest standard deviation (SD = 0.06). The importance of uranyl tris-carbonate is underlined by the smallest uncertainty in the log K value of all ternary complexes (SD = 0.04), followed by the contribution of $\equiv(\text{FeO-H})_2\text{UO}_2\text{CO}_3\text{OH}$ (SD = 0.07). In other words, these three uranyl surface species (Eqs. (1), (3), and (4)) are the most important for explaining the data set of Fig. 1, in combination with a bidentate carbonate complex (Eq. (2)) and polymer adsorption at very large concentrations (Eq. (5)).

4.3. Application of the derived model

The fitted model (Table 2) has been used to calculate the behavior of uranyl in the U(VI)-ferrihydrite systems of Wazne et al. (2003). The Fh was stored at 2 °C and used within 10 days. Nevertheless, the adsorption is predicted very well (Fig. 5). The U(VI) adsorption isotherm at pH = 5.9 of Jang et al. (2007) for Fh (aged for 4 days) could be described well with $A \sim 350 \text{ m}^2/\text{g}$. Note that the surface area A is substantially lower than for freshly prepared Fh. However, the adsorption isotherms at the higher pH values

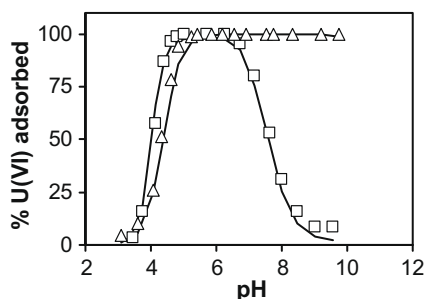


Fig. 5. The fractional uranyl adsorption in 0.01 M NaCl for closed systems with ferrihydrite (0.145 g/L, $A = 650 \text{ m}^2/\text{g}$) having 0.01 mM (triangles) or 10 mM (squares) total carbonate ($U_{\text{initial}} = 4.2 \mu\text{M}$). Data of Wazne et al. (2003). The lines are predictions based on the parameters given in Table 2 and Part I (Hiemstra and Van Riemsdijk, 2009).

(pH 6.8 and 7.8), where carbonate is strongly affecting the adsorption, could not be reproduced, being either too high ($\log U(\text{VI}) \sim <10^{-7} \text{ M}$) or too low ($\log U(\text{VI}) \sim >10^{-6} \text{ M}$). This may point to inconsistency with the isotherms derived by Morrison et al. at pH = 7 (Fig. 1). A possible reason might be due to the use of a uranyl stock solution that contained acetate, which could interfere and/or the use of only air as single source of carbonate.

The parameters found for the closed systems have also been used to predict adsorption in the open systems that were studied by Waite et al. (1994). The adsorption was predicted well for these systems using the parameters found for the closed system (Table 2) in combination with the parameters describing the primary charge (Hiemstra and Van Riemsdijk, 2009) as is shown by the lines in Fig. 2a–h. The description is good (RMSE = 0.27 log C–U(VI) units), which is not obvious since the sample has been aged for 3 days before use. Searching for the better estimate of the surface area by fitting it using the constants as given in Table 2 leads to $A = 510 \pm 30 \text{ m}^2/\text{g}$ (RMSE = 0.23 log C–U(VI) units). The lower surface area ($\sim 20\%$) is in line with the expectations.

5. DISCUSSION

The possible similarities between the structures of ferrihydrite and goethite invite us to speculate on the adsorption of uranyl by goethite. EXAFS data for ferrihydrite (Waite et al., 1994; Reich et al., 1998) indicate the presence of an Fe ion in the coordination shell at $\sim 342 \text{ pm}$. This distance is characteristic of edge sharing. Since edge-sharing by interaction of uranyl with a $\equiv\text{FeOH}^{-1/2}$ or $\equiv\text{Fe}_3\text{O}^{-1/2}$ group on the 110 faces of goethite is unlikely, a high U(VI) loading suggests that double-corner complex formation might be involved if binding of polymers with a U–U signature can be excluded by EXAFS. The expected Fe–U distance for a uranyl double-corner complex is about 420 pm. However, the spectrum does not show any intensity at this position. According to Sherman et al. (Sherman et al., 2008), the absence of a peak can be explained by a multiple scattering effect. This may imply that double-corner binding has not been identified in other cases, including ferrihydrite, for similar reasons. However, MO/DFT calculations (Sherman et al., 2008) suggest that a uranyl edge-sharing complex is much more stable than a double-corner complex. The calculated energy difference is large, $2\log K$ units. This implies that at low loading, edge sharing would be the dominant mechanism if both complexes can be formed. Moreover, the uranyl double-corner complex will experience more competition from the carbonate ion via site competition since both complexes occupy the same sites.

In our modeling of ferrihydrite, we could not find any contribution from this type of double-corner complex. A likely reason is that most data refer to a low loading and that the data obtained at a high U(VI) loading are affected by polymer formation. If the affinity of the edge-sharing complexes is relatively high, the measured adsorption on goethite will be strongly affected by the formation of this complex at a relatively low loading. Only at a high U(VI)

loading a significant contribution of double-corner complexes would be expected, and it is precisely under these conditions that polymer formation would obscure their role. The condition where the transition occurs will be determined by the number of edge sharing sites. This in turn will depend on the morphology of the goethite particles, in particular the needle length.

In the data analysis (Section 4), site densities have been used that we derived from surface structural considerations (Hiemstra and Van Riemsdijk, 2009). As described in Part I (Hiemstra and Van Riemsdijk, 2009), the largest uncertainty in the estimates was for the site density of the singly-coordinated surface groups that form the edges (FeOH(e)) of the octahedra as shown for the 001 face in Fig. 1 of Part I. It is possible to estimate the site density of this surface group by fitting the U(VI) adsorption data. However, adsorption is often more driven by electrostatic interactions than by site competition, which means that adsorption densities (adsorption maxima) are often poorly constrained by fitting alone. In our fit, the total site density was kept equal to the number (7.2 nm^{-2}) used to describe the surface charge (Hiemstra and Van Riemsdijk, 2009). This fitting resulted in $N_s(\text{FeOH(e)}) = 2.7 \pm 0.6 \text{ nm}^{-2}$. Within the uncertainties, this site density corresponds to the previously (Part I) estimated site density ($2.5 \pm 0.4 \text{ nm}^{-2}$) that has been used in our uranyl data analysis (Table 2).

Recently, a simple SCM has been proposed for the adsorption of uranyl by ferrihydrite, hematite, and goethite (Jang et al., 2007). The database for the uranyl solution chemistry used by these authors had been adapted and differs from the recent critical compilation of Guillaumont et al. (2003) used here. The SCM was based on the generalized two layer (GTL) model of Dzombak and Morel (1990) but had only one type of site. The estimated site density was much lower than found here with our structural approach. In the GTL model, adsorbed ions can only be located at the surface as a point charge. The linkage with the actual nature and configuration of surface species, as for example derived by spectroscopy, is almost absent. Besides the presence of adsorbed $\equiv\text{UO}_2\text{OH}^+$ and a $\equiv\text{U(VI)}$ polymer, the only ternary complex considered was adsorbed $\equiv\text{UO}_2\text{CO}_3$. The model was able to describe, in the absence of carbonate, the U(VI) adsorption isotherm of Morrison et al. (1995) at $\text{pH} = 7$ (Fig. 1c), but U(VI) adsorption in the presence carbonate (1.9 and 19.5 mM) was significantly underestimated. One of the possible reasons for this (amongst many others) might be the absence of a uranyl tris-carbonate surface species in their SCM.

The presence of a uranyl tris-carbonate surface species has recently been quantified using EXAFS data (Rossberg et al., 2009) for open systems in which the pH, partial pressure of CO_2 , and ionic strength were varied. The measured spectra were interpreted by principal component analysis and showed that the data could be largely explained by the presence of two types of surface species. Fitting of the EXAFS data to a structural model indicated the presence

of an edge-sharing uranyl surface complex and an adsorbed ternary type B surface complex with a local carbonate coordination close to that of aqueous $\text{UO}_2(\text{CO}_3)_3^{4-}$. The statistical analysis enabled the relative contribution of both complexes to be estimated. In a separate paper (Rossberg et al., 2009), we compare the abundance of the uranyl tris-carbonate surface complex predicted from the CD model with that derived from the EXAFS interpretation.

6. CONCLUSIONS

The above study can be summarized as follows:

The CD model is able to describe the uranyl adsorption in open and closed systems with a relatively small set of surface species over a very large range of conditions comprising $\text{pH} \approx 3\text{--}10$, $I \approx 0.01\text{--}0.5 \text{ M}$, $\text{CO}_3^{2-} \approx 0\text{--}20 \text{ mM}$, $\log[\text{U(VI)}] \approx -9$ to -4 , and a loading of $\approx 10^{-4}$ to 10^0 mol/kg .

The most remarkable surface species is a uranyl tris-carbonate surface complex. At relatively high pH and high carbonate concentrations, it can become the dominant surface species. For this complex, monodentate inner sphere complex formation is suggested.

A uranyl edge-sharing surface complex is also present. It may readily hydrolyze forming adsorbed $\equiv\text{UO}_2\text{OH}$. This species may also interact with CO_3^{2-} forming $\equiv\text{UO}_2\text{CO}_3\text{OH}$, a ternary type A surface complex. The overall contribution of these bidentate inner sphere complexes to the surface charge is probably $\Delta z_0 = 0.9 \pm 0.1 \text{ v.u.}$ The formation of a ternary type B uranyl-monocarbonato complex, i.e. $\equiv (\text{FeO})_2\text{COUO}_2(\text{OH})_3$ cannot be excluded. The type A or type B uranyl-monocarbonato complex is present at a relatively high pH but low carbonate concentrations. Finally, at very high uranyl concentrations, uranyl polymerizes at the surface of ferrihydrite making a detailed speciation difficult.

Aging of Fh for 3 days at 25°C may result in decrease of surface area of about 20% or more.

ACKNOWLEDGMENTS

We greatly appreciate the very valuable comments of David Kinniburgh. Additionally, the remarks of four other reviewers are gratefully acknowledged, all leading to a substantial improvement of this paper. We also thank the Associate Editor. K.-U.U. was supported by the U.S. Department of Energy, Office of Basic Energy Sciences Grant # 1027834 under the Master Grant DE-FG02-06ER64227. A. Rossberg was supported through the German Science Foundation (DFG) under Contract RO 2254/3-1.

APPENDIX A

See Table A1.

Table A1

Aqueous speciation reactions and their equilibrium constants ($I = 0$). For the uranium species, the reported uncertainty is given (\pm). See also http://migrationdb.jaea.go.jp/tdb_e/d_page_e/d_0500_e.html.

Species	Reaction	log K^a
UO_2OH^+	$1\text{UO}_2^{2+} + 1\text{H}_2\text{O} \leftrightarrow \text{UO}_2\text{OH}^+ + 1\text{H}^+$	-5.25 ± 0.25
$\text{UO}_2(\text{OH})_2^0$	$1\text{UO}_2^{2+} + 2\text{H}_2\text{O} \leftrightarrow \text{UO}_2(\text{OH})_2^0 + 2\text{H}^+$	-12.15 ± 0.07
$\text{UO}_2(\text{OH})_3^-$	$1\text{UO}_2^{2+} + 3\text{H}_2\text{O} \leftrightarrow \text{UO}_2(\text{OH})_3^- + 3\text{H}^+$	-20.25 ± 0.42
$\text{UO}_2(\text{OH})_4^{2-}$	$1\text{UO}_2^{2+} + 4\text{H}_2\text{O} \leftrightarrow \text{UO}_2(\text{OH})_4^{2-} + 4\text{H}^+$	-32.4 ± 0.68
$(\text{UO}_2)_2\text{OH}^{3+}$	$2\text{UO}_2^{2+} + 1\text{H}_2\text{O} \leftrightarrow (\text{UO}_2)_2\text{OH}^{3+} + \text{H}^+$	-2.7 ± 1.0
$(\text{UO}_2)_2(\text{OH})_2^{2+}$	$2\text{UO}_2^{2+} + 2\text{H}_2\text{O} \leftrightarrow (\text{UO}_2)_2(\text{OH})_2^{2+} + 2\text{H}^+$	-5.62 ± 0.04
$(\text{UO}_2)_3(\text{OH})_4^{2+}$	$3\text{UO}_2^{2+} + 4\text{H}_2\text{O} \leftrightarrow (\text{UO}_2)_3(\text{OH})_4^{2+} + 4\text{H}^+$	-11.90 ± 0.3
$(\text{UO}_2)_3(\text{OH})_5^+$ ^b	$3\text{UO}_2^{2+} + 5\text{H}_2\text{O} \leftrightarrow (\text{UO}_2)_3(\text{OH})_5^+ + 5\text{H}^+$	-15.55 ± 0.12
$(\text{UO}_2)_3(\text{OH})_7^-$	$3\text{UO}_2^{2+} + 7\text{H}_2\text{O} \leftrightarrow (\text{UO}_2)_3(\text{OH})_7^- + 7\text{H}^+$	-32.2 ± 0.8
$(\text{UO}_2)_4(\text{OH})_7^+$	$4\text{UO}_2^{2+} + 7\text{H}_2\text{O} \leftrightarrow (\text{UO}_2)_4(\text{OH})_7^+ + 7\text{H}^+$	-21.9 ± 1
UO_2CO_3^0	$1\text{UO}_2^{2+} + 1\text{CO}_3^{2-} \leftrightarrow \text{UO}_2\text{CO}_3^0$	$+9.94 \pm 0.03$
$\text{UO}_2(\text{CO}_3)_2^{2-}$	$1\text{UO}_2^{2+} + 2\text{CO}_3^{2-} \leftrightarrow \text{UO}_2(\text{CO}_3)_2^{2-}$	$+16.61 \pm 0.09$
$\text{UO}_2(\text{CO}_3)_3^{4-}$	$1\text{UO}_2^{2+} + 3\text{CO}_3^{2-} \leftrightarrow \text{UO}_2(\text{CO}_3)_3^{4-}$	$+21.84 \pm 0.04$
$(\text{UO}_2)_3(\text{CO}_3)_6^{6-}$	$3\text{UO}_2^{2+} + 6\text{CO}_3^{2-} \leftrightarrow (\text{UO}_2)_3(\text{CO}_3)_6^{6-}$	$+54 \pm 1$
$(\text{UO}_2)_2(\text{OH})_3(\text{CO}_3)^-$	$2\text{UO}_2^{2+} + 3\text{H}_2\text{O} + 1\text{CO}_3^{2-} \leftrightarrow (\text{UO}_2)_2(\text{OH})_3(\text{CO}_3)^- + 3\text{H}^+$	-0.86 ± 0.5
$(\text{UO}_2)_3(\text{OH})_3(\text{CO}_3)^+$	$3\text{UO}_2^{2+} + 3\text{H}_2\text{O} + 1\text{CO}_3^{2-} \leftrightarrow (\text{UO}_2)_3(\text{OH})_3(\text{CO}_3)^+ + 3\text{H}^+$	$+0.65 \pm 0.5$
$(\text{UO}_2)_{11}(\text{OH})_{12}(\text{CO}_3)_6^{2-}$	$11\text{UO}_2^{2+} + 12\text{H}_2\text{O} + 6\text{CO}_3^{2-} \leftrightarrow (\text{UO}_2)_{11}(\text{OH})_{12}(\text{CO}_3)_6^{2-} + 12\text{H}^+$	$+36.4 \pm 2$
UO_2NO_3^+	$1\text{UO}_2^{2+} + 1\text{NO}_3^- \leftrightarrow \text{UO}_2\text{NO}_3^+$	$+0.3 \pm 0.15$
UO_2Cl^+	$1\text{UO}_2^{2+} + 1\text{Cl}^- \leftrightarrow \text{UO}_2\text{Cl}^+$	$+0.17 \pm 0.02$
UO_2Cl_2^0	$1\text{UO}_2^{2+} + 2\text{Cl}^- \leftrightarrow \text{UO}_2\text{Cl}_2^0$	-1.1 ± 0.4
$\text{CO}_2(\text{g})^e$	$\text{CO}_3^{2-} + 2\text{H}^+ \leftrightarrow \text{H}_2\text{O}(\text{l}) + \text{CO}_2(\text{g})$	$+18.15$
$\text{H}_2\text{CO}_3^*^e$	$\text{CO}_3^{2-} + 2\text{H}^+ \leftrightarrow \text{H}_2\text{CO}_3^*$	$+16.69$
HCO_3^-	$\text{CO}_3^{2-} + 1\text{H}^+ \leftrightarrow \text{HCO}_3^-$	$+10.33$
$\text{NaHCO}_3^0^e$	$\text{CO}_3^{2-} + \text{Na}^+ + \text{H}^+ \leftrightarrow \text{NaHCO}_3^0$	$+10.14$
NaCO_3^-e	$\text{CO}_3^{2-} + \text{Na}^+ \leftrightarrow \text{NaCO}_3^-$	$+1.02$
$\text{Na}_2\text{CO}_3^0^e$	$\text{CO}_3^{2-} + 2\text{Na}^+ \leftrightarrow \text{Na}_2\text{CO}_3^0$	$+0.01$
NaCl^0^c	$\text{Na}^+ + \text{Cl}^- \leftrightarrow \text{NaCl}^0$	-0.80
$\text{NaNO}_3^0^d$	$\text{Na}^+ + \text{NO}_3^- \leftrightarrow \text{NaNO}_3^0$	-0.60
$\text{H}_2\text{O}(\text{l})$	$\text{H}^+ + \text{OH}^- \leftrightarrow \text{H}_2\text{O}(\text{l})$	$+14.00$
$\text{UO}_2(\text{OH})_2(\text{s})$	$\text{UO}_2(\text{OH})_2(\text{s}) + 2\text{H}^+ \leftrightarrow \text{UO}_2^{2+} + 2\text{H}_2\text{O}(\text{l})$	$+5.3 \pm 0.3$

^a For U(VI) from Guillaumont et al. (2003).

^b Might also be represented as $(\text{UO}_2)_3\text{O}(\text{OH})_3^+$ (Tsushima et al., 2007).

^c From Sverjensky et al. (1997).

^d From Smith and Martell (1981).

^e From Rahnemaie et al. (2007).

REFERENCES

- Arai Y., McBeath M., Bargar J. R., Joye J. and Davis J. A. (2006) Uranyl adsorption and surface speciation at the imogolite–water interface: self-consistent spectroscopic and surface complexation models. *Geochim. Cosmochim. Acta* **70**(10), 2492–2509.
- Bargar J. R., Kubicki J. D., Reitmeyer R. and Davis J. A. (2005) ATR-FTIR spectroscopic characterization of coexisting carbonate surface complexes on hematite. *Geochim. Cosmochim. Acta* **69**(6), 1527–1542.
- Bargar J. R., Reitmeyer R. and Davis J. A. (1999) Spectroscopic confirmation of uranium (VI)-carbonato adsorption complexes on hematite. *Environ. Sci. Technol.* **33**, 2481–2484.
- Bargar J. R., Reitmeyer R., Lenhart J. J. and Davis J. A. (2000) Spectroscopic characterization of U(VI)-carbonato surface complexes on hematite: EXAFS and electromobility measurements. *Geochim. Cosmochim. Acta* **64**(16), 2737–2749.
- Barnett M. O., Jardine P. M. and Brooks S. C. (2002) U(VI) adsorption to heterogeneous subsurface media: application of a surface complexation model. *Environ. Sci. Technol.* **36**(5), 937–942.
- Bostick B. C., Fendorf S., Barnett M. O., Jardine P. M. and Brooks S. C. (2002) Uranyl surface complexes formed on subsurface media from DOE facilities. *Soil Sci. Soc. Am. J.* **66**(1), 99–108.
- Brown I. D. (2002) *The Chemical Bond in Inorganic Chemistry: The Bond Valence Model*. Oxford University Press.
- Brown I. D. and Altermatt D. (1985) Bond-valence parameters obtained from a systematic analysis of the inorganic crystal structure database. *Acta Cryst.* **B41**, 244–247.
- Burns P. C., Ewing R. C. and Hawthorne F. C. (1997) The crystal chemistry of hexavalent uranium: polyhedron geometries, bond-valence parameters, and polymerization of polyhedra. *Can. Mineral.* **35**, 1551–1570.
- Catalano J. G., Trainor T. P., Eng P. J., Waychunas G. A. and Brown G. E. (2005) CTR diffraction and grazing-incidence EXAFS study of U(VI) adsorption onto alpha- Al_2O_3 and alpha- Fe_2O_3 (1–102) surfaces. *Geochim. Cosmochim. Acta* **69**(14), 3555–3572.
- Cheng T., Barnett M. O., Roden E. E. and Zhunag J. L. (2007) Reactive transport of uranium(VI) and phosphate in a goethite-coated sand column: an experimental study. *Chemosphere* **68**(7), 1218–1223.
- Davis J. A., Meece D. E., Kohler M. and Curtis G. P. (2004) Approaches to surface complexation modeling of uranium(VI) adsorption on aquifer sediments. *Geochim. Cosmochim. Acta* **68**(18), 3621–3641.
- Dodge C. J., Francis A. J., Gillow J. B., Halada G. P., Eng C. and Clayton C. R. (2002) Association of uranium with iron oxides

- typically formed on corroding steel surfaces. *Environ. Sci. Technol.* **36**(16), 3504–3511.
- Dzombak D. A. and Morel F. M. M. (1990) *Surface Complexation Modeling: Hydrous Ferric Oxide*. John Wiley & Sons: New York. p. 393.
- Gabriel U., Gaudet J. P., Spadini L. and Charlet L. (1998) Reactive transport of uranyl in a goethite column: an experimental and modelling study. *Chem. Geol.* **151**(1–4), 107–128.
- Guillaumont R., Fanghänel T., Neck V., Fuger J., Palmer D.A., Grenthe I. and Rand M. H. (2003) *Update on the Chemical Thermodynamics of Uranium, Neptunium, Plutonium, Americium and Technetium*. Elsevier.
- Hiemstra T., Rahnemaie R. and Van Riemsdijk W. H. (2004) Surface complexation of carbonate on goethite: IR spectroscopy, structure and charge distribution. *J. Colloid Interf. Sci.* **278**, 282–290.
- Hiemstra T. and Van Riemsdijk W. H. (1990) Multiple activated complex dissolution of metal (hydr)oxides: a thermodynamic approach applied to quartz. *J. Colloid Interf. Sci.* **136**(1), 132–150.
- Hiemstra T. and Van Riemsdijk W. H. (1996) A surface structural approach to ion adsorption: the charge distribution (CD) model. *J. Colloid Interf. Sci.* **179**, 488–508.
- Hiemstra T. and Van Riemsdijk W. H. (1999) Surface structural ion adsorption modeling of competitive binding of oxyanions by metal (hydr)oxides. *J. Colloid Interf. Sci.* **210**, 182–193.
- Hiemstra T. and Van Riemsdijk W. H. (2006) On the relationship between charge distribution, surface hydration and the structure of the interface of metal hydroxides. *J. Colloid Interf. Sci.* **301**, 1–18.
- Hiemstra T. and Van Riemsdijk W. H. (2007) Adsorption and surface oxidation of Fe(II) on metal (hydr)oxides. *Geochim. Cosmochim. Acta* **71**(24), 5913–5933.
- Hiemstra T. and Van Riemsdijk W. H. (this issue) A surface structural model for ferrihydrite I: sites related to primary charge, molar mass, and mass density. *Geochim. Cosmochim. Acta*.
- Hsi C.-K. D. and Langmuir D. (1985) Adsorption of uranyl onto ferric oxyhydroxides: application of the surface complexation site-binding model. *Geochim. Cosmochim. Acta* **49**, 1931–1941.
- Jang J. H., Dempsey B. A. and Burgos W. D. (2007) A model-based evaluation of sorptive reactivities of hydrous ferric oxide and hematite for U(VI). *Environ. Sci. Technol.* **41**(12), 4305–4310.
- Keizer M. G. and Van Riemsdijk W. H. (1998) ECOSAT, Equilibrium Calculation of Speciation and Transport. Technical Report Department Soil Quality. Wageningen University.
- Kinniburgh D. G. (1993) Fit, Technical Report WD/93/23. British Geological Survey.
- LaViolette R. A. and Redden G. D. (2002) Comment on “modeling the mass-action expression for bidentate adsorption”. *Environ. Sci. Technol.* **36**(10), 2279–2280.
- Logue B. A., Smith R. W. and Westall J. C. (2004) U(VI) adsorption on natural iron-coated sands: comparison of approaches for modeling adsorption on heterogeneous environmental materials. *Appl. Geochem.* **19**(12), 1937–1951.
- Manceau A., Charlet L., Boisset M. C., Didier B. and Spadini L. (1992) Sorption and speciation of heavy metals on hydrous Fe and Mn oxides. From microscopic to macroscopic. *Appl. Clay Sci.* **7**, 201–223.
- Morrison S. J., Spangler R. R. and Tripathi V. S. (1995) Adsorption of uranium(VI) on amorphous ferric oxyhydroxide at high-concentrations of dissolved carbon(IV) and sulfur(VI). *J. Contam. Hydrol.* **17**(4), 333–346.
- Oda Y. and Aoshima A. (2002) Ab initio quantum chemical study on charge distribution and molecular structure of uranyl (VI) species with Raman frequency. *J. Nucl. Sci. Technol.* **39**(6), 647–654.
- Payne T. E. (1999) Uranium (VI) interactions with mineral surfaces: controlling factors and surface complexation modeling, University of New South Wales.
- Payne T. E., Davis J. A. and Waite T. D. (1994) Uranium retention by weathered schists – the role of iron minerals. *Radiochim. Acta* **66-7**, 297–303.
- Payne T. E., Lumpkin G. R. and Waite T. D. (1998) Uranium (VI) adsorption on model minerals: controlling factors and surface complexation modeling. In *Adsorption of Metals by Geomedia* (ed. E. A. Jenne). Academic Press.
- Rahnemaie R., Hiemstra T. and Van Riemsdijk W. H. (2007) Carbonate adsorption on goethite in competition with phosphate. *J. Colloid Interf. Sci.* **315**(2), 415–425.
- Reich T., Moll H., Arnold T., Denecke M. A., Hennig C., Geipel G., Bernhard G., Nitsche H., Allen P. G., Bucher J. J., Edelstein N. M. and Shuh D. K. (1998) An EXAFS study of uranium(VI) sorption onto silica gel and ferrihydrite. *J. Electron Spectrosc.* **96**(1–3), 237–243.
- Rietra R. P. J. J., Hiemstra T. and Van Riemsdijk W. H. (1999) The relationship between molecular structure and ion adsorption on variable charge minerals. *Geochim. Cosmochim. Acta* **63**(19/20), 3009–3015.
- Rosentreter J. J., Swantje Quarder H., Smith R. W. and McLing T. (1998) Uranium sorption onto natural sands as a function of sediment characteristics and solution pH. In *Adsorption of Metals by Geomedia* (ed. E. A. Jenne). Academic Press.
- Rossberg A., Ulrich K. U., Weiss S., Tsushima S., Hiemstra T. and Scheinost A. C. (2009) Identification of uranyl surface complexes on ferrihydrite: advanced EXAFS data analysis and CD-MUSIC modelling. *Environ. Sci. Technol.* **43**(5), 1400–1406.
- Sherman D. M., Peacock C. L. and Hubbard C. G. (2008) Surface complexation of U(VI) on goethite (alpha-FeOOH). *Geochim. Cosmochim. Acta* **72**(2), 298–310.
- Smith R. M. and Martell A. E. (1981) *Critical Stability Constants*. Plenum.
- Stachowicz M., Hiemstra T. and Van Riemsdijk W. H. (2006) Surface speciation of As(III) and As(V) adsorption in relation to charge distribution. *J. Colloid Interf. Sci.* **302**, 62–75.
- Stachowicz M., Hiemstra T. and van Riemsdijk W. H. (2008) Multi-competitive interaction of As(III) and As(V) oxyanions with Ca²⁺, Mg²⁺, PO₄³⁻, and CO₃²⁻ ions on goethite. *J. Colloid Interf. Sci.* **320**(2), 400–414.
- Sverjensky D. A., Shock E. L. and Helgeson H. C. (1997) Prediction of the thermodynamic properties of aqueous metal complexes to 1000 degrees C and 5 kb. *Geochim. Cosmochim. Acta* **61**(7), 1359–1412.
- Tsushima S., Rossberg A., Ikeda A., Muller K. and Scheinost A. C. (2007) Stoichiometry and structure of uranyl(VI) hydroxo dimer and trimer complexes in aqueous solution. *Inorg. Chem.* **46**(25), 10819–10826.
- Ulrich K. U., Rossberg A., Foerstendorf H., Zanker H. and Scheinost A. C. (2006) Molecular characterization of uranium(VI) sorption complexes on iron(III)-rich acid mine water colloids. *Geochim. Cosmochim. Acta* **70**(22), 5469–5487.
- Vandenhove H., Van Hees M., Wannijn J., Wouters K. and Wang L. (2007) Can we predict uranium bioavailability based on soil parameters? Part 2: soil solution uranium concentration is not a good bioavailability index. *Environ. Pollut.* **145**(2), 577–586.
- Waite T. D., Davis J. A., Payne T. E., Waychunas G. A. and Xu N. (1994) Uranium(VI) adsorption to ferrihydrite: application of a surface complexation model. *Geochim. Cosmochim. Acta* **58**, 5465–5478.

Wazne M., Korfiatis G. P. and Meng X. G. (2003) Carbonate effects on hexavalent uranium adsorption by iron oxyhydroxide. *Environ. Sci. Technol.* **37**(16), 3619–3624.

Zachara J. M., Girvin D. C., Schmidt R. L. and Resch C. T. (1987) Chromate adsorption on amorphous iron oxyhydroxide in the

presence of major groundwater ions. *Environ. Sci. Technol.* **21**(6), 589–594.

Associate editor: Kevin M. Rosso